

PDF model based on Langevin equation for polydispersed two-phase flows applied to a bluff-body gas-solid flow

Jean-Pierre Minier¹, Eric Peirano² and Sergio Chibbaro³

¹Electricité de France, Div. R&D, MFTT, 6 Quai Watier, 78400 Chatou, France
E-mail: Jean-Pierre.Minier@edf.fr

²ADEME-DER, 500 Route des Lucioles 06560 Valbonne France
E-mail: eric.peirano@ademe.fr

³Institut Jean Le Rond D'Alembert Universit Pierre et Marie Curie
E-mail: sergio.chibbaro@upmc.fr

November 8, 2018

Abstract

The aim of the paper is to discuss the main characteristics of a complete theoretical and numerical model for turbulent polydispersed two-phase flows, pointing out some specific issues. The theoretical details of the model have already been presented [Minier and Peirano, Physics Reports, Vol. 352/1-3, 2001]. Consequently, the present work is mainly focused on complementary aspects, that are often overlooked and that require particular attention. In particular, the following points are analysed : the necessity to add an extra term in the equation for the velocity of the fluid seen in the case of two-way coupling, the theoretical and numerical evaluations of particle averages and the fulfilment of the particle mass-continuity constraint. The theoretical model is developed within the PDF formalism. The important-physical choice of the state vector variables is first discussed and the model is then expressed as a stochastic differential equation (SDE) written in continuous time (Langevin equations) for the velocity of the fluid seen. The interests and limitations of Langevin equations, compared to the single-phase case, are reviewed. From the numerical point of view, the model corresponds to an hybrid Eulerian/Lagrangian approach where the fluid and particle phases are simulated by different methods. Important aspects of the Monte Carlo particle/mesh numerical method are emphasised. Finally, the complete model is validated and its performance is assessed by simulating a bluff-body case with an important recirculation zone and in which two-way coupling is noticeable.

1 Introduction

Dispersed two-phase flows, where a continuous phase (a gas or a liquid) carries discrete particles (solid particles, droplets, bubbles, . . .), are of great interest in environmental studies and engineering applications, such as dispersion of small particles in the atmosphere or combustion of fuel droplets in a car engine.

To simulate these flows, the basic equations must be written: the Navier-Stokes equations for the fluid phase and the momentum equation for a single particle embedded in a turbulent flow, the latter issue still being a subject of current research. For small particle-based Reynolds numbers Re_p (whose definition is specified below) and particle diameters that are of the same order of magnitude as the Kolmogorov length scale, a general form of the particle momentum equation has been proposed [1, 2].

In the present work, only heavy particles ($\rho_p \gg \rho_f$) are under consideration and the equations of

motion for a particle can be written:

$$\frac{d\mathbf{x}_p}{dt} = \mathbf{U}_p, \quad (1a)$$

$$\frac{d\mathbf{U}_p}{dt} = \frac{1}{\tau_p}(\mathbf{U}_s - \mathbf{U}_p) + \mathbf{g}, \quad (1b)$$

where $\mathbf{U}_s = \mathbf{U}(\mathbf{x}_p(t), t)$ is the fluid velocity seen, *i.e.* the fluid velocity sampled along the particle trajectory $\mathbf{x}_p(t)$, not to be confused with the fluid velocity $\mathbf{U}_f = \mathbf{U}(\mathbf{x}_f(t), t)$ denoted with the subscript f . The particle relaxation time is defined as

$$\tau_p = \frac{\rho_p}{\rho_f} \frac{4d_p}{3C_D|\mathbf{U}_r|}, \quad (2)$$

where the local instantaneous relative velocity is $\mathbf{U}_r = \mathbf{U}_p - \mathbf{U}_s$ and the drag coefficient C_D is a non-linear function of the particle-based Reynolds number, $Re_p = d_p|\mathbf{U}_r|/\nu_f$, which means that C_D is a complicated function of d_p , the particle diameter [3]. A very often retained empirical form for the drag coefficient is

$$C_D = \begin{cases} \frac{24}{Re_p} [1 + 0.15Re_p^{0.687}] & \text{if } Re_p \leq 1000, \\ 0.44 & \text{if } Re_p \geq 1000. \end{cases} \quad (3)$$

In the present work, attention is focused on some aspects of the problem. In particular, only dilute incompressible gas-particle flows are considered, so that particle-particle interactions are neglected but two-way coupling is retained, which means that particle dispersion and modulation of turbulence by the particles are accounted for.

The complete problem is formed by the discrete particle equations given above, Eqs (1) to (3) and the field equations of the fluid phase, the continuity and the Navier-Stokes equations, supplemented with a source term \mathbf{S} that represents the force exerted by the particles on the fluid

$$\frac{\partial U_{f,j}}{\partial x_j} = 0, \quad (4a)$$

$$\frac{\partial U_{f,i}}{\partial t} + U_{f,j} \frac{\partial U_{f,i}}{\partial x_j} = -\frac{1}{\rho_f} \frac{\partial P}{\partial x_i} + \nu \frac{\partial^2 U_{f,i}}{\partial x_j^2} + S_i. \quad (4b)$$

An “exact approach” (in the spirit of DNS) is possible [4], but in practice, the exact equations of motion are not of great help. Indeed, in the case of a large number of particles and of turbulent flows at high Reynolds numbers, the number of degrees of freedom is huge and one has to resort to a contracted probabilistic description.

Following the classical approach used in single-phase turbulence, one can think of writing directly mean-field equations for a limited number of particle statistics (mean velocity, kinetic energy, ...) as in $k - \epsilon$ or $R_{ij} - \epsilon$ modelling. This is the basis of the Eulerian approach [5, 6]. However, due to the complex dependence of τ_p on particle diameters and on fluid and particle instantaneous velocities, the drag term represents a non-linear but local (in term of particle variables) source term. The resulting closure problem that appears in the Eulerian approach is therefore difficult. Actually, this issue is very similar to the one appearing in the modelling of single-phase turbulent reactive flows [7] and, in this case, PDF models that can treat the reactive source terms without approximation have shown their great potential. For the same reason, a PDF approach to polydispersed turbulent two-phase flows is interesting. In practice, mean-field equations ($R_{ij} - \epsilon$) are used for the fluid whereas a particle pdf equation is solved by a Monte Carlo method using a trajectory point of view (Eulerian/Lagrangian models). The PDF model is therefore formulated as a particle stochastic Lagrangian model (a set of SDEs).

Numerous Eulerian/Lagrangian two-phase flow models have been proposed (most of the time with interesting and clear ideas), but often with a discrete formulation (in time) and without making the connection with a PDF model. When Eulerian/Eulerian (*i.e.* both phases are described with mean-field equations) and Eulerian/Lagrangian models are compared directly, the PDF framework is helpful to reveal that these

methods do not contain the same level of information: Lagrangian models are PDF models from which Eulerian models can be extracted in a consistent way [6, 8]. The specificity of the present work is to present a Lagrangian model, based on a Langevin equation for the velocity of the fluid seen, in the PDF context. The theoretical formulation of the Langevin PDF model has already been developed [8, 9] and the purpose of the present paper is to give an overview of the complete theoretical and numerical issues insisting on complementary points. In the same PDF framework, an alternative formulation consists in writing a PDF equation in analogy with Boltzmann kinetic equation [10], that is only for particle location and velocity, without considering directly the velocity of the fluid seen. For a comprehensive review of general results and methods in particle dispersion, we refer also to Stock's paper [11].

More specifically, the aims of the present paper are:

- (i) to outline the main aspects of a PDF model, the interests and limitations of current state-of-the-art Langevin models and the keys points of numerical algorithms,
- (ii) to point-out and to address new specific issues for Lagrangian models, such as the addition of extra terms for two-way coupling, numerical averages and the mean-continuity constraint,
- (iii) to validate the complete model and to show how it performs by comparing the numerical results with experimental ones in a practical case.

The paper is organised as follows: in Section 2, several mathematical notions related to stochastic modelling are clarified, that is the equivalence between the trajectory and pdf points of view, and the modelling strategy which is adopted in the present work (the particle-tracking approach). The dimension of the system, that is the dimension of the state vector, is also given based on physical principals. In Section 3, closure proposals are put forward for the fluid velocity seen, in the form of Langevin equations. Emphasis is put on the terms to be added in order to model cases with two-way coupling. In Section 4, the numerical approach is presented. The main steps of the particle-mesh algorithm are explained, while particular attention is devoted to the problems of defining averages in two-phase flows and of verifying the particle mean-continuity constraint. These models are validated in the simulation of a practical case of gas-solid flows, Section 5.

2 Stochastic modelling

2.1 Mathematical background

In this section, basic results, concerning the mathematical background of the approach and the correspondence between SDEs and Fokker-Planck equations, are recalled [7, 12, 13]. If one considers a system of N particles interacting through forces that can be expressed as functions of variables attached to each particle (for example, position, velocity, ...), then all available information is contained in the state vector, \mathbf{Z} , of the complete system

$$\mathbf{Z} = (Z_1^1, Z_2^1, \dots, Z_p^1; Z_1^2, Z_2^2, \dots, Z_p^2; \dots; Z_1^N, Z_2^N, \dots, Z_p^N), \quad (5)$$

where Z_j^i represents the j -variable attached to the particle labelled i . The dimension of the state vector is then $d = N \times p$ where N is the total number of particles and p the number of variables attached to each particle. The complete system, that is the N -particles, is closed. In classical mechanics, the time evolution of such systems is often described by a set of ordinary differential equations

$$\frac{d\mathbf{Z}}{dt} = \mathbf{A}(t, \mathbf{Z}), \quad (6)$$

which corresponds, in sample space, to the Liouville equation [12]

$$\frac{\partial p(t, \mathbf{z})}{\partial t} + \frac{\partial}{\partial \mathbf{z}} (\mathbf{A}(t, \mathbf{z}) p(t, \mathbf{z})) = 0, \quad (7)$$

for the associated pdf, $p(t, \mathbf{z})$. This formulation is similar to a pure convection problem (first-order partial derivatives in sample space).

As mentioned in the previous section, most of the time, the number of degrees of freedom (the dimension of the state vector) is huge and one has to resort to a reduced (or contracted) description [13]. Consequently, one-particle pdf, $p(t, \mathbf{z}^i)$ (for a particle i) or two-particle pdf, $p(t, \mathbf{z}^i, \mathbf{z}^j)$, etc. can be considered instead of choosing the N -particle pdf, $p(t, \mathbf{z})$. Let \mathbf{Z}^R be a reduced state vector (typically a one-particle state vector $\mathbf{Z}^R = (Z_1, Z_2, \dots, Z_p)$ corresponding to the p variables attached to each particle). Then, the time evolution equations, in physical space, for this sub-system have the form:

$$\frac{d\mathbf{Z}^R}{dt} = \mathbf{A}(t, \mathbf{Z}^R, \mathbf{Y}), \quad (8)$$

where there is a dependence on the external variable \mathbf{Y} (related to the particles not contained in \mathbf{Z}^R). In sample space, the marginal pdf $p^r(t, \mathbf{z}^r)$ verifies

$$\frac{\partial p^r(t, \mathbf{z}^r)}{\partial t} + \frac{\partial}{\partial \mathbf{z}^r} [\langle \mathbf{A} | \mathbf{z}^r \rangle p^r(t, \mathbf{z}^r)] = 0, \quad (9)$$

where the conditional expectation is defined by

$$\langle \mathbf{A} | \mathbf{z}^r \rangle = \int \mathbf{A}(t, \mathbf{z}^r, \mathbf{y}) p(\mathbf{y} | t, \mathbf{z}^r) d\mathbf{y} = \frac{1}{p(t, \mathbf{z}^r)} \int \mathbf{A}(t, \mathbf{z}^r, \mathbf{y}) p(t, \mathbf{z}^r, \mathbf{y}) d\mathbf{y}. \quad (10)$$

Eq. (9) is now unclosed, showing that a reduced description of a system implies a loss of information and the necessity to introduce a model.

In the present paper, and for reasons presented in the next section, the reduced system will be modelled by stochastic diffusion processes [7, 9, 12, 14]. For such stochastic processes, the time-evolution equations for the trajectories of the process are SDEs written as:

$$dZ_i^R = A_i(t, \mathbf{Z}^R(t)) dt + B_{ij}(t, \mathbf{Z}^R(t)) dW_j, \quad (11)$$

where $W_j = (W_1, \dots, W_n)$ is a set of independent Wiener processes [14] and n is the dimension of the reduced state vector. In Eq. (11), $\mathbf{A} = (A_i)$ is called the drift vector and $\mathbf{B} = (B_{ij})$ the diffusion matrix. SDEs require a strict mathematical definition of the stochastic integral [12, 14] which is defined here in the *Itô sense* (these equations are referred to as Langevin equations in the physical literature). The corresponding equation in sample space for $p^r(t, \mathbf{z}^r)$ is the Fokker-Planck equation

$$\frac{\partial p^r}{\partial t} = - \frac{\partial}{\partial z_i^r} [A_i(t, \mathbf{z}^r) p^r] + \frac{1}{2} \frac{\partial^2}{\partial z_i^r \partial z_j^r} [D_{ij}(t, \mathbf{z}^r) p^r]. \quad (12)$$

where $D_{ij} = B_{il} B_{lj} = (BB^*)_{ij}$ is a positive-definite matrix. In a weak sense (when one is only interested in statistics of the process), one can speak of an equivalence between SDEs and Fokker-Planck equations.

2.2 Dimension of the state vector

The dimension of the reduced state vector, \mathbf{Z}^R , that is the number of particles N and the number of attached variables p for each particle, have to be determined (hereafter the upper-scripts r and R are dropped for the sake of simplicity). The first choice for N is done in line with current state-of-the-art models for single-phase flows [7]. Indeed, when the particle relaxation time τ_p is small, particles behave as fluid particles. In single-phase turbulence [15], only one-particle PDF models are sufficiently general to be applicable to complex flows. For this reason, our first choice is to retain a one-particle pdf description for the particle phase in the two-phase flows under consideration here ($N = 1$).

The second choice is to select the specific variables attached to the solid particles. Again, a closer look at single-phase PDF models [7] might be helpful. In single-phase flows at high Reynolds numbers, Kolmogorov theory [16] tells us that, for a reference time scale dt in the inertial range, Lagrangian increments of the fluid velocity are well correlated whereas increments of the fluid acceleration are nearly uncorrelated. This indicates that for dt belonging to the inertial range, the fluid velocity is a slow variable and the fluid acceleration is a fast variable which can be eliminated (fast variable elimination) [17]. Therefore, the state

vector should include position and velocity, *i.e.* $(\mathbf{x}_f, \mathbf{U}_f)$ ($p = 2$). This is the starting point for Langevin equation models for fluid particle velocities [15, 18]. The model takes the form of a diffusion process with a drift term linear in the velocity of the fluid seen [18]

$$dx_{f,i} = U_{f,i} dt, \quad (13)$$

$$dU_{f,i} = -\frac{1}{\rho_f} \frac{\partial \langle P \rangle}{\partial x_i} dt + G_{ij}(U_{f,i} - \langle U_{f,i} \rangle) dt + \sqrt{C_0 \langle \epsilon \rangle} dW_i, \quad (14)$$

where $\langle P \rangle$ is the mean pressure field, $\langle \epsilon \rangle$ is the mean dissipation rate and C_0 is a constant given by Kolmogorov theory ($C_0 = 2.1$). G_{ij} is a matrix which depends on mean quantities,

$$G_{ij} = -\frac{1}{T_L} \delta_{ij} + G_{ij}^a. \quad (15)$$

where G_{ij}^a is an anisotropy matrix (depending on mean quantities) and T_L stands for a timescale given by (k is the turbulent kinetic energy)

$$T_L = \frac{1}{\left(\frac{1}{2} + \frac{3}{4}C_0\right)} \frac{k}{\langle \epsilon \rangle}. \quad (16)$$

In the two-phase flow case, a similar reasoning [9] suggests to include the velocity of the fluid seen in the state vector that becomes (the fluid acceleration seen is a fast variable)

$$\mathbf{Z} = (\mathbf{x}_p, \mathbf{U}_p, \mathbf{U}_s). \quad (17)$$

This is different from the choice made in analogy to Boltzmann equation, when one considers only $\mathbf{Z} = (\mathbf{x}_p, \mathbf{U}_p)$ as in kinetic models [19, 20]. Yet, we are dealing with particles being agitated by an underlying turbulent fluid and a (slow) variable related to the fluid, namely the velocity of the fluid seen, is explicitly kept in the state vector. With the kinetic choice, not only the derivatives of the fluid velocity seen have to be modelled but also the fluid velocity seen itself.

3 Modelling turbulent dispersion

With the present choice of the state vector, the stochastic process used to describe the system has been chosen, *i.e.* $\mathbf{Z} = (\mathbf{x}_p, \mathbf{U}_p, \mathbf{U}_s)$. Following the trajectory point of view mentioned in Section 2.1, a time-evolution equation for \mathbf{U}_s has to be proposed. This equation, together with Eqs (1), will give the complete system of SDEs for the components of \mathbf{Z} . Contrary to most Lagrangian models, which are often built in a discrete setting, the current model is written in continuous time, as Eq. (11), in order to be consistent with the proposed mathematical framework.

From the physical point of view, a time-evolution equation for \mathbf{U}_s amounts to modelling turbulent dispersion, an issue which is more complicated than turbulent diffusion. Indeed, particle inertia (τ_p) and the effect of an external force field induce a separation of the fluid element and of the discrete particle initially located at the same point, as represented in Fig. 1. In the asymptotic limit of small particle inertia, $\tau_p \rightarrow 0$, and in absence of external forces, this separation effect disappears and the problem of modelling diffusion is retrieved, for which the stochastic model given by Eq. (14) can be applied. For that reason, dispersion models (simulation of \mathbf{U}_s) are extensions of diffusion models (simulation of \mathbf{U}_f).

An extensive description of the physical aspects of turbulent dispersion has been proposed elsewhere [9, 21], so that only the key points used to derive the stochastic model are recalled in the next section. It is proposed to consider separately the physical effects of particle inertia and external forces. Two non-dimensional numbers have been introduced for that purpose: particle inertia is measured by the Stoke number $St = \tau_p/T_L$, and external forces by $\xi = |U_r|/u'$, u' being a characteristic fluid turbulent velocity ($u' = \sqrt{2k/3}$). The influence of these two effects on the characteristics of \mathbf{U}_s are :

- (i) in the absence of external forces ($\xi = 0$), only particle inertia plays a role. The characteristic, or integral, timescale of the velocity of the fluid seen, say $T_L^*(\xi = 0)$ is expected to vary between the fluid Lagrangian timescale, T_L , in the limit of low St numbers, and the Eulerian timescale, T_E , in the limit of high St numbers.

- (ii) Leaving out particle inertia, external forces creates mean drifts ($\xi \neq 0$) and induce a decorrelation of the velocity of the fluid seen with respect to the velocity of fluid particles. This effect is called the crossing trajectory effect (CTE) and is related to a mean relative velocity between particles and the fluid rather than an instantaneous one.

In the model developed in the present paper, it is assumed that T_E remains of the same order of magnitude as T_L , which seems actually a reasonable choice since there is little information for complex flows. Detailed models have been proposed for the effect of particle inertia [21], but in the following it will be neglected, that is $T_L^*(\xi = 0) = T_L$. The representative picture is now sketched in Fig. 2 where only the mean drift induces separation.

3.1 Langevin equation model

Using the physical description of the CTE effect as due to a mean-drift (Fig. 2), Kolmogorov theory can be applied, as in the single-phase case, to suggest a dispersion model. Indeed, let us introduce $\mathbf{v}(\tau, \mathbf{r}) = \mathbf{u}_f(t_0 + \tau, \mathbf{x}_0 + \mathbf{u}(t_0, \mathbf{x}_0)\tau + \mathbf{r}) - \mathbf{u}_f(t_0, \mathbf{x}_0)$, the fluid velocity field relative to the velocity of the fluid particle F at time t_n , Fig. 2, that is with $\mathbf{u}_f(t_0, \mathbf{x}_0) = \mathbf{u}_s(t_0)$, then one can write that

$$d\mathbf{U}_s = \mathbf{v}(dt, \langle \mathbf{U}_r \rangle dt), \quad (18)$$

where $\langle \mathbf{U}_r \rangle = \langle \mathbf{U}_p \rangle - \langle \mathbf{U}_s \rangle$ is the mean relative velocity between the discrete particle and the surrounding fluid element. Then, the differential change, and so the Eulerian statistics, of the fluid velocity seen depend on the key variables of Kolmogorov (as the fluid velocity), that is $\langle \epsilon \rangle$ and ν , and on the mean drift due to the CTE effect, but not on the instantaneous particle or fluid velocities. Since it is the mean velocity \mathbf{U}_r that appears in Eq. (18), the Kolmogorov theory can then be applied [16], to show that for high-Reynolds number flows and for a time increment dt that belongs to the inertial range, we have

$$\langle dU_{s,i} dU_{s,j} \rangle = D_{ij}(dt), \quad (19)$$

where the matrix D_{ij} is determined by the two scalars functions $D_{||}$ and D_{\perp} through

$$D_{ij} = D_{\perp} \delta_{ij} + [D_{||} - D_{\perp}] r_i r_j, \quad (20)$$

the separation vector \mathbf{r} being in the direction of the mean relative velocity, $\mathbf{r} = \langle \mathbf{U}_r \rangle / |\langle \mathbf{U}_r \rangle|$. The functions $D_{||}$ and D_{\perp} are the longitudinal and transverse velocity correlation, respectively. Dimensional analysis yields that in the inertial range, one can write

$$D_{||}(dt) = \langle \epsilon \rangle dt \alpha_{||} \left(\frac{|\langle \mathbf{U}_r \rangle|^2}{\langle \epsilon \rangle dt} \right), \quad D_{\perp}(dt) = \langle \epsilon \rangle dt \alpha_{\perp} \left(\frac{|\langle \mathbf{U}_r \rangle|^2}{\langle \epsilon \rangle dt} \right). \quad (21)$$

For the two functions $\alpha_{||}$ and α_{\perp} , there is no exact prediction, but in two limit cases they can be explicitly computed. On one hand, when the mean relative velocity is small, $|\langle \mathbf{U}_r \rangle| \ll (\langle \epsilon \rangle dt)^{1/2}$, for a given time interval dt , the statistics of the velocity of the fluid seen are expected to be close to the fluid ones, and thus $\alpha_{||} \simeq \alpha_{\perp} \simeq C_0$. On the other hand, when the mean relative velocity is large, ($|\langle \mathbf{U}_r \rangle| \gg (\langle \epsilon \rangle dt)^{1/2}$), one can resort to the frozen turbulence hypothesis, and in that case (C is a constant)

$$D_{||}(dt) \simeq C \langle \epsilon \rangle \langle \mathbf{U}_r \rangle dt^{2/3}, \quad D_{\perp}(dt) \simeq \frac{4}{3} C \langle \epsilon \rangle \langle \mathbf{U}_r \rangle dt^{2/3}, \quad (22)$$

which shows that, in that limit, the two functions $\alpha_{||}(x)$ and $\alpha_{\perp}(x)$ vary as $x^{1/3}$. Then, the Langevin model is not supported as in the fluid case, since it will always give a velocity correlation linear in time for each components of D . Nevertheless, a useful approximation can be proposed. Indeed, if we freeze the values of the functions $\alpha_{||}$ and α_{\perp} for a certain value of the time interval, say Δt_r , and write

$$D_{||}(dt) \simeq \langle \epsilon \rangle dt \alpha_{||} \left(\frac{|\langle \mathbf{U}_r \rangle|^2}{\langle \epsilon \rangle \Delta t_r} \right), \quad D_{\perp}(dt) \simeq \langle \epsilon \rangle dt \alpha_{\perp} \left(\frac{|\langle \mathbf{U}_r \rangle|^2}{\langle \epsilon \rangle \Delta t_r} \right), \quad (23)$$

a linear variation of $D_{\parallel}(dt)$ and $D_{\perp}(dt)$, with respect to the time interval dt , is now obtained. The reference time lag may be the Lagrangian timescale which is the timescale over which fluid velocities are correlated. And since $\langle \epsilon \rangle T_L \simeq k$, we have

$$D_{\parallel}(dt) \simeq \langle \epsilon \rangle dt \alpha_{\parallel} \left(\frac{|\langle \mathbf{U}_r \rangle|^2}{k} \right), \quad D_{\perp}(dt) \simeq \langle \epsilon \rangle dt \alpha_{\perp} \left(\frac{|\langle \mathbf{U}_r \rangle|^2}{k} \right). \quad (24)$$

This result suggests now a Langevin equation model which consists in simulating \mathbf{U}_s as a diffusion process. As explained above, this model is only an approximate model having less support than in the fluid case. Indeed, the Langevin model does not yield the correct spectrum (in the limit of large relative velocity or frozen turbulence). However, for engineering purposes, where the macroscopic behaviour is the real subject of interest, the important properties are the integral time scales rather than the precise form of the spectrum. Thus, Langevin models are “reasonable compromises” between simplicity and physical accuracy at the moment. It is also clear that much work remains to be done to improve stochastic models.

It can be shown [9] that the general stochastic differential equations for the fluid velocity seen process have the form (\mathbf{X} stands for fluid fields)

$$dU_{s,i} = A_i(t, \mathbf{Z}, \langle \mathbf{Z} \rangle, \langle \mathbf{X} \rangle) dt + B_{ij}(t, \mathbf{Z}, \langle \mathbf{Z} \rangle, \langle \mathbf{X} \rangle) dW_j, \quad (25)$$

where the drift vector, \mathbf{A}_s , and the diffusion matrix, \mathbf{B}_s , have the form

$$\begin{aligned} dU_{s,i} = & -\frac{1}{\rho_f} \frac{\partial \langle P \rangle}{\partial x_i} dt + (\langle U_{p,j} \rangle - \langle U_{f,j} \rangle) \frac{\partial \langle U_{f,i} \rangle}{\partial x_j} dt \\ & - \frac{1}{T_{L,i}^*} (U_{s,i} - \langle U_{f,i} \rangle) dt \\ & + \sqrt{\langle \epsilon \rangle} \left(C_0 b_i \tilde{k} / k + \frac{2}{3} (b_i \tilde{k} / k - 1) \right) dW_i. \end{aligned} \quad (26)$$

The CTE has been modelled by changing the timescales in drift and diffusion terms according to Csanady’s analysis. Assuming, for the sake of simplicity, that the mean drift is aligned with the first coordinate axis (the general case is discussed elsewhere [9]), the modelled expressions for the timescales are, in the longitudinal direction

$$T_{L,1}^* = \frac{T_L^*(\xi = 0)}{\sqrt{1 + \beta^2 \frac{|\langle \mathbf{U}_r \rangle|^2}{2k/3}}}, \quad (27)$$

and in the transversal directions (axes labelled 2 and 3)

$$T_{L,2}^* = T_{L,3}^* = \frac{T_L^*(\xi = 0)}{\sqrt{1 + 4\beta^2 \frac{|\langle \mathbf{U}_r \rangle|^2}{2k/3}}}. \quad (28)$$

In these equations β is the ratio of the Lagrangian and the Eulerian timescales of the fluid, $\beta = T_L/T_E$, and $T_L^*(\xi = 0)$ represents the Lagrangian time-scale in the absence of mean drifts but accounting for particle inertia. As mentioned at the end of the previous section, particle inertia effect are neglected in the present work [21] and we therefore assume that $T_L^*(\xi = 0) = T_L$. In the diffusion matrix, a new kinetic energy has been introduced ($b_i = T_L/T_{L,i}$)

$$\tilde{k} = \frac{3}{2} \frac{\sum_{i=1}^3 b_i \langle u_{f,i}^2 \rangle}{\sum_{i=1}^3 b_i}. \quad (29)$$

In the absence of mean drifts, the stochastic model for \mathbf{U}_s reverts to the Langevin equation model used in single-phase PDF modelling [7] and is thus free of any spurious drift by construction. Finally, it must be emphasised that the derivation of a satisfactory model (that is respecting a number of well-established constraints) for particle dispersion remains an open issue.

3.2 Modelling two-way coupling

In order to account for the influence of the particles on the fluid, a new term is added in the momentum equation of the fluid velocity, see Eqs (4), and the fluid velocity seen,

$$dU_{s,i} = [A_{s,i}(t, \mathbf{Z}, \langle \mathbf{Z} \rangle, \langle \mathbf{X} \rangle) + A_{p \rightarrow s,i}(t, \mathbf{Z}, \langle \mathbf{Z} \rangle)] dt + B_{s,ij}(t, \mathbf{Z}, \langle \mathbf{Z} \rangle, \langle \mathbf{X} \rangle) dW_j. \quad (30)$$

The exact expression for this acceleration, $A_{p \rightarrow s,i}(t, \mathbf{Z}, \langle \mathbf{Z} \rangle)$, which is induced by the presence of the discrete particles, is not a priori known. The underlying force corresponds to the exchange of momentum between the fluid and the particles, but should not be confused with the total force acting on particles since the latter includes external forces such as gravity. The effect of particles on fluid properties is expressed directly in the stochastic equation of \mathbf{U}_s with a simple stochastic model. The force exerted by one particle on the fluid corresponds to the drag force written here as

$$\mathbf{F}_{p \rightarrow f} = -m_p \frac{\mathbf{U}_s - \mathbf{U}_p}{\tau_p}, \quad (31)$$

where m_p is the mass of a particle. The total force acting on the fluid element surrounding a discrete particle is then obtained as the sum of all elementary forces, $\mathbf{F}_{p \rightarrow f}$, and the resulting acceleration is modelled here as [9]

$$A_{p \rightarrow s,i} = -\frac{\alpha_p \rho_p}{\alpha_f \rho_f} \frac{U_{p,i} - U_{s,i}}{\tau_p}. \quad (32)$$

Eq. (30) is justified by the assumption that the mean transfer rate of energy and energy dissipation $\langle \epsilon \rangle$ is changed by the presence of particles, but the nature and structure of turbulence remains the same. Therefore, Eq. (30) is written by adding an acceleration term, $\mathbf{A}_{p \rightarrow s}$, to account for the presence of particles, while the same closures as in the one-way coupling case will be used for the drift vectors and the diffusion matrices, where, once again, the mean fields $\langle \epsilon \rangle, \langle U_f^2 \rangle, \dots$ are modified by the presence of the particles. Indeed, the drift vectors and the diffusion matrices not being affected by the nature of turbulence, remain unchanged. In opposition to the previous hypotheses, recent results of direct numerical simulations in the field of turbulence modulation by particles (in isotropic turbulence) [4] seem to indicate that there is a non-uniform distortion of the energy spectrum. This could mean that, contrary to our previous assumption, the nature and structure of the energy transfer mechanisms of turbulence are modified by the presence of particles. There is no precise 'geometrical' knowledge on the structure of turbulence in the presence of discrete particles and this makes it extremely difficult to isolate the important variables in order to modify the theory of Kolmogorov (which is used in our closures). This problem is out of the scope of the present paper and it remains an open question. Then, the final set of equations for the velocity of the fluid seen are:

$$\begin{aligned} dU_{s,i} = & -\frac{1}{\rho_f} \frac{\partial \langle P \rangle}{\partial x_i} dt + (\langle U_{p,j} \rangle - \langle U_{f,j} \rangle) \frac{\partial \langle U_{f,i} \rangle}{\partial x_j} dt - \frac{\alpha_p \rho_p}{\alpha_f \rho_f} \frac{U_{p,i} - U_{s,i}}{\tau_p} dt \\ & - \frac{1}{T_{L,i}^*} (U_{s,i} - \langle U_{f,i} \rangle) dt \\ & + \sqrt{\langle \epsilon \rangle} \left(C_0 b_i \tilde{k}/k + \frac{2}{3} (b_i \tilde{k}/k - 1) \right) dW_i. \end{aligned} \quad (33)$$

It is seen that the resulting Langevin equation, which is believed to represent the simplest model for two-phase flows, contains a diagonal but non-isotropic diffusion matrix, $B_{s,ij} = B_{s,i} \delta_{ij}$. It is also worth emphasising that the closure relations put forward just above reflect modelling choices. For instance, in the two-phase flow case, the isotropic form of the diffusion matrix cannot be obtained anymore, but it is *chosen* to select among different possibilities, a diagonal diffusion matrix.

3.3 Equivalence with the PDF approach

According to the arguments developed in Section 2.1, the complete set of SDEs (for the state vector $\mathbf{Z} = (\mathbf{x}_p, \mathbf{U}_f, \mathbf{U}_s)$),

$$dx_{p,i} = U_{p,i} dt \quad (34a)$$

$$dU_{p,i} = \frac{1}{\tau_p} (U_{s,i} - U_{p,i}) dt + g_i dt \quad (34b)$$

$$dU_{s,i} = [A_{s,i}(t, \mathbf{Z}, \langle \mathbf{Z} \rangle, \langle \mathbf{X} \rangle) + A_{p \rightarrow s,i}(t, \mathbf{Z}, \langle \mathbf{Z} \rangle)] dt + B_{s,ij}(t, \mathbf{Z}, \langle \mathbf{Z} \rangle, \langle \mathbf{X} \rangle) dW_j. \quad (34c)$$

is equivalent to a Fokker-Planck equation given in closed form for the corresponding pdf $p(t; \mathbf{y}_p, \mathbf{V}_p, \mathbf{V}_s)$ which is, in sample space

$$\begin{aligned} \frac{\partial p}{\partial t} + V_{p,i} \frac{\partial p}{\partial y_{p,i}} = & - \frac{\partial}{\partial V_{p,i}} (A_{p,i} p) \\ & - \frac{\partial}{\partial V_{s,i}} ([A_{s,i} + \langle A_{p \rightarrow s,i} | \mathbf{y}_p, \mathbf{V}_p, \mathbf{V}_s \rangle] p) + \frac{1}{2} \frac{\partial^2}{\partial V_{s,i} \partial V_{s,j}} ([B_s B_s^T]_{ij} p). \end{aligned} \quad (35)$$

The equation for the Eulerian pdf and the resulting mean-field equations can be found in [8].

4 Numerical Issues

The theoretical model developed in Section 3 represents a PDF model for the particle phase only. It does not contain any description of the continuous phase. It is possible to extend the PDF description to both the fluid and particle phases [8], which may be useful for theoretical and consistency analysis. However, at the moment, this complete PDF approach is limited for practical calculations, and, in the present work, a classical second-moment approach is followed for the continuous phase. The complete numerical model is therefore an hybrid method and corresponds to a classical approach referred to as Eulerian/Lagrangian in the literature, as mentioned in Section 1. As one can see from Section 3, the terminology is not actually adequate to describe the complete model (it would be better to talk of a Moment/PDF hybrid approach), but corresponds to the numerical approach. Indeed, from the numerical point of view, the fluid phase is modelled by mean fields, obtained by solving partial differential equations on a grid with an Eulerian approach, while the particle phase is modelled by a large number of Lagrangian particles distributed in the domain and whose properties are obtained by solving stochastic differential equations. It is worth emphasising that these particles are now stochastic particles, or more precisely samples of the underlying pdf, rather than precise models of the actual particles. The overall numerical method is therefore an example of Monte Carlo particle-mesh techniques.

The numerical (particle-mesh) approach involves many issues. Some of them have already been treated in classical textbooks [22], but only for deterministic equations. The stochastic nature of the present equations brings in specific aspects and raises new questions. In that respect, the purpose of this section is not to give a comprehensive description of all issues. It is more to give an overview of the numerical method, pointing out important issues and, in particular, those that, in our opinion, require additional work. More precisely, issues that have not always been investigated or may have been overlooked (such as consistent discrete averages, Section 4.3, and mass-continuity constraint, Section 4.4), are developed more in detail.

4.1 General Algorithm

The flow-chart of the code is shown in Fig. 3. At each time step, the fluid mean fields are first computed by solving the corresponding partial differential equations (RSM model) with a classical finite volume approach. The Eulerian solver then provides the Lagrangian solver with the fluid mean fields that are necessary to advance particles properties. In the Lagrangian solver, the dispersed phase is represented by a large number of particles and, as proposed by the model, the state vector attached to each particle is $\mathbf{Z} = (\mathbf{x}_p, \mathbf{U}_f, \mathbf{U}_s)$. Once particle properties have been updated, and in the case of two-way coupling,

where particles modify the fluid flow, source terms accounting for momentum and energy exchange between the two phases are also calculated and are fed back into the Eulerian solver for the next time step computation. It is then seen that the two solvers are only loosely-coupled. This may lead to numerical difficulties when the particle loading is increased, consequently the source terms become important and the system of equations stiff. However, our present aim is to model moderate particle loading phenomena, indeed particle-particle collisions have been neglected. In that range, particles can still modify the fluid flow in a noticeable way but source terms remain small enough so that the loosely-coupled algorithm can still be retained.

As previously explained, the particle properties are modelled by a vectorial SDE written as

$$dZ_i = A_i(t, \mathbf{Z}, \langle f(\mathbf{Z}) \rangle, \langle \mathbf{X} \rangle)dt + B_{ij}(t, \mathbf{Z}, \langle f(\mathbf{Z}) \rangle, \langle \mathbf{X} \rangle)dW_j \quad (36)$$

where f is a general function depending on the model and \mathbf{X} stands for fluid fields. It is worth emphasising that the drift and diffusion coefficients depend on statistics derived from the pdf that is implicitly calculated. Therefore, these SDEs are different from standard ones [14, 26]. Updating particles properties implies three steps: (i) projection of $\langle f(\mathbf{Z}) \rangle$ and $\langle \mathbf{X} \rangle$ at particle positions, (ii) time integration of Eq. (36), and (iii) averaging to compute the new values of $\langle f(\mathbf{Z}) \rangle$ (for stationary flows, such as the one considered later on, ensemble averages computed in every cell are then averaged in time, once the stationary regime has been reached. This time-averaging procedure is very helpful to reduce statistical noise to a negligible level [23–25]). Since averaging is basically the reverse operation of projection [22], these three steps correspond to two main issues:

- (i) the first concerns the derivation of accurate numerical schemes for the time integration of Eq. (36). Due to the non-linear nature of the equations, this is still a difficult point [26, 27] and, moreover, physical constraints should be respected [28]. This issue is briefly developed below.
- (ii) The second issue is related to the exchange of information between the grid-based Eulerian variables, located at cell centres and particles which are continuously distributed in the domain. At the moment, a NGP (nearest grid point) technique [22] is used, this represents the simplest choice but also the best one in terms of spatial error [23]. This is an important and attractive issue to investigate for particle-mesh methods with in the case of unstructured meshes and taking into account boundary conditions.

4.2 Time-integration of SDEs

Since we are interested in the numerical approximation of statistics derived from particles, a weak numerical scheme [27] (converging in law) is under consideration. A numerical scheme is said to be of order of convergence r in time, in the weak sense, if, for any sufficiently smooth function

$$|\langle f(\mathbf{Z}) \rangle - \langle f(\mathbf{Z}^{\Delta t}) \rangle| \leq C (\Delta t)^r, \quad (37)$$

where C is a constant and $\mathbf{Z}^{\Delta t}$ represents the numerical approximation of \mathbf{Z} . The numerical scheme used in the present calculations is detailed in [28], and consequently, in the present paper, only some points of particular importance are emphasised. Eq. (36) must be understood in the *Itô sense* and it is fundamental that numerical schemes respect the Itô definition of the stochastic integral, in order to avoid any inconsistency problems [29]. The weak numerical scheme is of order 2 in time, unconditionally stable but still explicit [28]. Another important issue is the numerical fulfilment of physical limits [9]. Indeed, in practical engineering calculations of complex flows, it may occur that, locally, one has $\Delta t \gg \tau_p$, or even $\Delta t \gg T^*, \tau_p$, that is the time-step becomes much larger than the characteristic time scales of the system, Eqs (34). In the first case, one should have that $\mathbf{U}_p \rightarrow \mathbf{U}_s$ and, in the second case, the model expresses a pure diffusive behaviour in space [9, 28]

$$dx_{p,i} = \langle x_{f,i} \rangle dt + (B_{s,ij} T_L^*)dW_i. \quad (38)$$

It is important that the numerical scheme is consistent with these continuous limits.

4.3 Discrete representation and numerical averages

Since averages are fundamental in the construction of PDF models, it is useful to clarify the correspondence between the averages (defined as the mathematical expectations) and Monte Carlo estimations, which are used in the code. In polydispersed cases, even when ρ_p is constant, the mass of each particle can be different because of different diameters. This suggests that even for constant density particles, the natural definition or understanding of a mean quantity is the *mass-weighted* average. This kind of choice is somewhat analogous to the Favre mean definition for compressible single-phase fluid flows.

To justify this, we start by introducing a Lagrangian mass density function $F^L(t; \mathbf{y}_p, \mathbf{V}_p, \Psi_p)$ where

$$F^L(t; \mathbf{y}_p, \mathbf{V}_p, \Psi_p) d\mathbf{y}_p d\mathbf{V}_p d\Psi_p, \quad (39)$$

is the probable mass of discrete particles in an infinitesimal volume in sample space. As a matter of fact, attention is focused on Eulerian averages (at a point (t, \mathbf{x}_p) fixed in time and space), for which the analogous Eulerian mass density function is defined by

$$\begin{aligned} F^E(t, \mathbf{x}; \mathbf{V}_p, \psi_p) &= F^L(t; \mathbf{y}_p = \mathbf{x}, \mathbf{V}_p, \psi_p) \\ &= \int F^L(t; \mathbf{y}_p, \mathbf{V}_p, \psi_p) \delta(\mathbf{x} - \mathbf{y}_p) d\mathbf{y}_p, \end{aligned} \quad (40)$$

where F^E is normalised by $\langle \rho_p \rangle$ (is the expected density)

$$\alpha_p(t, \mathbf{x}) \langle \rho_p \rangle(t, \mathbf{x}) = \int F^E(t, \mathbf{x}; \mathbf{V}_p, \psi_p) d\mathbf{V}_p d\psi_p. \quad (41)$$

α_p represents the probability to find particles at a given time and position, in any state. The Eulerian mass density function being defined, we can introduce a general average for a quantity $H(\mathbf{U}(t), \phi(t))$

$$\alpha_p(t, \mathbf{x}) \langle \rho_p \rangle(t, \mathbf{x}) \langle H_p \rangle(t, \mathbf{x}) = \int H_p(\mathbf{V}_p, \Psi_p) F^E(t, \mathbf{x}; \mathbf{V}_p, \Psi_p) d\mathbf{V}_p d\psi_p. \quad (42)$$

The Lagrangian mass density function can be written from a discrete point of view as

$$F_N^L(t; \mathbf{y}_p, \mathbf{V}_p, \psi_p) = \sum_{i=1}^N m^i \delta(\mathbf{y}_p - \mathbf{x}_p^i(t)) \otimes \delta(\mathbf{V}_p - \mathbf{U}_p^i(t)) \otimes \delta(\psi_p - \phi_p^i(t)) \quad (43)$$

where m^i is the mass of the particle labelled i and N is the number of samples. From Eq. (39), the discrete Eulerian mass-density functions is

$$F_N^E(t, \mathbf{x}_p; \mathbf{V}_p, \psi_p) = \frac{1}{\delta\mathcal{V}_x} \sum_{i=1}^N m^i \delta(\mathbf{V}_p - \mathbf{U}_p^i(t)) \otimes \delta(\psi_p - \phi_p^i(t)), \quad (44)$$

$\delta\mathcal{V}_x$ being a small volume around point \mathbf{x} . Then, a numerical approximation of Eq. (41) is

$$\alpha_p(t, \mathbf{x}) \langle \rho_p \rangle \simeq \frac{\sum_{i=1}^N m_p^i}{\delta\mathcal{V}_x}, \quad (45)$$

and the numerical approximation of a particle mean quantity is

$$\langle H_p \rangle \simeq H_{p,N} = \frac{\sum_{i=1}^N m_p^i H_p(\mathbf{U}_p^i(t), \phi_p^i(t))}{\sum_{i=1}^N m_p^i}. \quad (46)$$

Convergence of the discrete approximation is ensured by the Central Limit Theorem which shows that there exists a constant C such that, when $N \rightarrow +\infty$,

$$\langle H_{p,N} \rangle = \langle H_p \rangle \quad \text{and} \quad \langle (\langle H_p \rangle - H_{p,N})^2 \rangle \leq \frac{C}{N_x}. \quad (47)$$

It is therefore seen that the convergence of the underlying pdf is not in a strong sense but in a weak sense, or to be more precise in law [14], since it is in fact the mean value of functions of the stochastic process \mathbf{Z} that converges as $N \rightarrow +\infty$,

$$H_{N,p} = \langle H(\mathbf{Z}_N) \rangle \xrightarrow{N \rightarrow \infty} \langle H(\mathbf{Z}) \rangle. \quad (48)$$

4.4 Pressure correction

It has been shown in Section 3.3 that there is a correspondence SDE - Fokker-Planck equation. From the pdf equation, mean particle fields can then be extracted [8]. In other words, every particle stochastic model is consistent with a certain Eulerian model [6,9] as in single-phase PDF models [30].

With the definition of the mean particle velocity field given in the previous section, the corresponding particle continuity equation is (density is constant)

$$\frac{\partial}{\partial t}(\alpha_p \rho_p) + \frac{\partial}{\partial x_i}(\alpha_p \rho_p \langle U_{p,i} \rangle) = 0. \quad (49)$$

For each time step in the Lagrangian solver, the mean fields α_p and $\langle \tilde{U}_{p,i} \rangle$ are computed from particle location and velocity, \mathbf{x}_p and \mathbf{U}_p , using the numerical approximations given in Eqs (45) and (46). Here, we propose to modify particle velocities (not locations) so as to enforce the mean continuity constraint, by adding a pressure-correction field as a potential ϕ . The corrected particle velocity field is then

$$\langle U_{p,i} \rangle = \langle \tilde{U}_{p,i} \rangle - \frac{\partial \phi}{\partial x_i}, \quad (50)$$

where ϕ is calculated from the Poisson equation

$$\frac{\partial}{\partial x_i}(\alpha_p \rho_p \frac{\partial \phi}{\partial x_i}) = \frac{\partial}{\partial t}(\alpha_p \rho_p) + \frac{\partial}{\partial x_i}(\alpha_p \rho_p \langle \tilde{U}_{p,i} \rangle). \quad (51)$$

The mean velocity correction term is then applied to each particle velocity.

This pressure-correction term used here for the particle velocity is of course similar to the classical pressure-correction step applied in the Eulerian solver for the fluid. Yet, it is often overlooked in Lagrangian calculations. If we consider the complete algorithm, it is then seen that there are now two pressure-correction steps due to the two mean-continuity equations, one for the fluid and one for the particles. This is also a consequence of the loosely-coupled algorithm.

5 Numerical investigation

5.1 Experimental setup

The experimental setup is typical for pulverised coal combustion where primary air and coal are injected in the centre and secondary air is introduced on the periphery, Fig. 4.

This is a typical bluff-body flow where the gas (air at ambient temperature, $T = 293 K$) is injected in the inner region and also in the outer region where the inlet velocity is high enough to create a recirculation zone downstream of the injection (two honeycombs were used in the experiment in order to stabilise the flow so that no swirl was present). Solid particles (glass particles of density $\rho_p = 2450 kg/m^3$) are then injected from the inner cylinder with a given mass flow rate and from there interact with the gas turbulence. This is a coupled turbulent two-phase flow since the particle mass loading at the inlet is high enough (22%) for the particles to modify the fluid mean velocities and kinetic energy. This is also a polydispersed flow where particle diameters vary according to a known distribution at the inlet, typically between $d_p = 20 \mu m$ and $d_p = 110 \mu m$ around an average of $d_p \sim 60 \mu m$.

Experimental data are available for radial profiles (the flow is stationary and axi-symmetric) of different statistical quantities at five axial distances downstream of the injection ($x = 0.08, 0.16, 0.24, 0.32$ and 0.40 m). These quantities include the mean axial and radial velocities as well as the fluctuating radial and axial velocities for both the fluid and the particle phase. Axial profiles along the axis of symmetry for these quantities have also been measured. All the data was gathered using PDA measurement techniques. Further details on the experimental setup and the measurement techniques can be found in Ishima *et al.* [31].

The 'Hercule' experimental setup is a very interesting test case for two-phase flow modelling and numerical simulations where most of the different aspects of two-phase flows are present. The particles are dispersed by the turbulent flow but in return modify this one. Furthermore, the existence of a recirculation

zone where particles interact with negative axial fluid velocities constitutes a much more stringent test case compared to cases where the fluid and the particle mean velocities are of the same sign (the problem is then mostly confined to radial dispersion issues).

5.2 Results and discussion

All the results were obtained by using the ESTET 3.4 software on a HP-C3000 workstation. In all numerical computations, the axi-symmetry property was used: a two-dimensional curvilinear mesh with $74 \times 3 \times 142$ nodes was generated. The sensitivity to the various parameters of the numerical investigation was accurately studied. In particular, independence with respect to the time step was checked. A uniform time step, $\Delta t = 10^{-3}$ s, was then used in all computations.

The computations were carried out with a $R_{ij} - \epsilon$ turbulence model, which is based on the standard IPM model [32, 33]. Actually, this choice is satisfying from the point of view of the consistency with the stochastic model. It is known that there is a rigorous correspondence between the Lagrangian stochastic models and the second-order closures in the case of turbulent single-phase flows [30].

In the two-phase flow calculations, particles were injected when the single-phase flow stationary regime was reached (as the limit of the unstationary regime) before the introduction of the discrete particles in the domain. About 1000 time steps were computed for the single-phase problem. Around 400 to 500 additional time steps were needed to reach the stationary regime for the two-phase flow situation (around 14000 particles were at this stage present in the domain). Statistics extracted from the particle data set were then averaged in time (for about 1000 time steps) to reduce the statistical noise.

The computational performances are shown in Table 1. Normally, Lagrangian algorithms require much more computational time than the Eulerian eddy-viscosity models [9]. In this case, for the same number of computational elements (either mesh points or nodes), they appear comparable. The computational requirements for the Eulerian solver is increased due to the use of a full second-order turbulence model which implies the numerical resolution of 6 coupled partial differential equations for the fluctuating velocities (added to the 3 equations for the mean momentum) compared to only 1 for eddy-viscosity models.

The experimental set of measures provides data both along the axis and in cross sections at various points in the domain. The comparison is made in all directions and at all cross sections of measures. The cross section at $x = 0.16$ is located within the recirculation zone while the cross section at $x = 0.4$ is located downstream of the limit of the recirculation zone.

The overall agreement between experimental data and the computed profiles is good. In particular, the particle fluctuating velocity is well reproduced both in shape and in magnitude.

In Fig. 5 and 6, the mean fluid and particle velocities along the axis are shown. It is noticeable that the comparison between the computed results and the experimental findings for the two-phase flow in presence of two-way coupling is worse than in single-phase computation. The same effect characterises both the mean fluid and the particle profiles. They results less well reproduced in two domain zones, although the qualitatively agreement remains good. The point of recirculation is overestimated and the velocity slope after it is underestimated. This effects indicates the necessity of further studies on the coupling between particles and the fluid. It is worth noting that these effects are limited to the behaviour along the axis. In Fig. 8-10 first two statistical moments of the particles velocity ($\langle U_p \rangle$, $\langle W_p \rangle$, $\sqrt{\langle u_p'^2 \rangle}$) are shown, without smoothing. The difference between experimental data and computed results at the axis ($x = 0$) does not influence the computation in the rest of the domain. In Fig. 7 we show the profiles of the fluid mean axial velocity, where an analogous behaviour is present, with a satisfactory agreement in the whole domain except the values on the axis.

6 Conclusions

In this paper, a theoretical and numerical model for particle turbulent polydispersed two-phase flows has been presented. The theoretical model is a PDF model and, in practice, appears as a Lagrangian stochastic model. It consists in the simulation of a large number of stochastic particles which simulate the behaviour of real particles dispersed in the fluid. Each particle is defined by a set of variables and the selection of these state variables represents an important choice from the physical point of view. At present, the

state variables attached to each particle include particle position, particle velocity and the fluid velocity seen. The present model is developed as a diffusion stochastic process for the velocity of the fluid seen. This is similar to single-phase turbulence, but the extension to the two-phase flow case requires additional assumptions in the application of the Kolomogorov hypotheses, as detailed in Section 3. A specific point is that, in the case of two-way coupling, an extra term is needed in the stochastic equation for the velocity of the fluid seen in order to be consistent with the mean field equations for the fluid phase.

From the numerical point of view, an hybrid Eulerian/Lagrangian, or moment/Monte Carlo, approach is discussed. At each time step, the fluid phase is computed with an Eulerian code which provides the Lagrangian module with mean fluid quantities. The particles are then tracked and source terms representing the momentum and kinetic energy exchanges are evaluated to be included in the Reynolds stress equations. This corresponds to a classical approach, but new aspects have been emphasized. In particular, apart from considerations on numerical schemes and the evaluation of particle means, the necessity of a correction to satisfy particle continuity equation has been stressed.

The interests and capabilities of the model have been illustrated by the computation of a test case representative of an engineering situation. Numerical predictions are in good agreement with the experimental ones and can be regarded as a validation of the model.

Some of the current developments to this work aim at improving numerical aspects (variance reduction technique for the computational efficiency, new methods to compute statistical averages) and at improving the physics of the model in the near-wall region (boundary layer).

7 Acknowledgements

We would like to thank Dr. Mehdi Ouraou for his fruitful collaboration in numerical simulations.

References

- [1] R. Gatignol. The Faxén formulae for a rigid particle in an unsteady non-uniform Stokes flow. *Journal de Mécanique Théorique et Appliquée*, 1(2):143–160, 1983.
- [2] Maxey M.R. and Riley J.J. Equation of motion for a small rigid sphere in a nonuniform flow. *Phys. Fluids*, 26(4):883–889, 1983.
- [3] R. Clift, J. R. Grace, and M. E. Weber. *Bubbles, Drops and Particles*. Academic Press, New York, 1978.
- [4] M. Boivin, O. Simonin, and K. D. Squires. Direct numerical simulation of turbulence modulation by particles in isotropic turbulence. *J. Fluid Mech.*, 375:235–263, 1998.
- [5] O. Simonin, E. Deutsch, and J-P. Minier. Eulerian prediction of the fluid/particle correlated motion in turbulent two-phase flows. *Applied Scientific Research*, 51:275–283, 1993.
- [6] O. Simonin. Continuum modelling of dispersed two-phase flows. *Combustion and Turbulence in Two-Phase Flows, Lecture Series Programme, Von Karman Institute*, 1996.
- [7] S. B. Pope. *Turbulent Flows*. Cambridge University Press, 2000.
- [8] E. Peirano and J-P. Minier. A probabilistic formalism and hierarchy of models for polydispersed turbulent two-phase flows. *Phys. Rev. E*, 65(046301):1–18, 2002.
- [9] J-P. Minier and E. Peirano. The PDF approach to polydispersed turbulent two-phase flows. *Physics Reports*, 352(1–3):1–214, 2001.
- [10] F. Mashayek and R.V.R. Pandya. Analytical Description of Particle/Droplet-Laden Turbulent Flows. *Progress in Energy and Combustion Science*, 29 (4):329-378, 2003.
- [11] D.E. Stock. Particle dispersion in flowing gases. *J. Fluids Eng.*, 118:4-17, 1996.

- [12] C. W. Gardiner. *Handbook of Stochastic Methods for Physics, Chemistry and the Natural Sciences*. Springer-Verlag, Berlin, 2nd edition, 1990.
- [13] R. Balescu. *Statistical dynamics: matter out of equilibrium*. Imperial College Press, London, 1997.
- [14] L. Arnold. *Stochastic Differential Equations: Theory and Applications*. Wiley, New-York, 1974.
- [15] S. B. Pope. Lagrangian pdf methods for turbulent reactive flows. *Ann. Rev. Fluid Mechanics*, 26:23–63, 1994.
- [16] A. S. Monin and A. M. Yaglom. *Statistical Fluid Mechanics*. MIT Press, Cambridge, Mass, 1975.
- [17] H. Haken. Synergetics: an overview. *Rep. Prog. Phys.*, 52:515–533, 1989.
- [18] J-P. Minier and J. Pozorski. Derivation of a pdf model for turbulent flows based on principles from statistical physics. *Phys. Fluids*, 9(6):1748–1753, 1997.
- [19] M. W. Reeks. On the continuum equations for dispersed particles in nonuniform flows. *Phys. Fluids A*, 4(6):1290–1303, 1992.
- [20] R.V.R. Pandya and F. Mashayek. Non-isothermal dispersed phase of particles in turbulent flow. *J. of Fluid Mech.*, 475:205–245, 2003.
- [21] J. Pozorski and J-P. Minier. On the lagrangian turbulent dispersion models based on the langevin equation. *Int. J. of Multiphase Flow*, 24:913–945, 1998.
- [22] R. W. Hockney and J. W. Eastwood. *Computer simulation using particles*. Adam Hilger, New-York, 1988.
- [23] J. Xu and S. B. Pope. Assessment of numerical accuracy of PDF/Monte-Carlo methods for turbulent reacting flows. *J. Comp. Phys.*, 152:192, 1999.
- [24] P. Jenny, S.B. Pope, M. Muradoglu, and D.A. Caughey. A hybrid algorithm for the joint PDF equation of turbulent reactive flows. *J. Comput. Phys.*, 166:218–252, 2001.
- [25] P. Jenny, M. Muradoglu, K. Liu, S.B. Pope, and D. A. Caughey. Pdf simulations of a bluff-body stabilized flow. *J. Comput. Phys.*, 169:1–23, 2001.
- [26] D. Talay. *Simulation of Stochastic Differential Equation, in Probabilistic Methods in Applied Physics*. Springer-Verlag, Berlin, 1995. P. Kree and W. Wedig.
- [27] P.E. Kloeden and E. Platen. *Numerical solution of stochastic differential equations*. Springer-Verlag, Berlin, 1992.
- [28] J-P. Minier, E. Peirano, and S. Chibbaro. Weak first- and second order numerical schemes for stochastic differential equations appearing in lagrangian two-phase flow modelling. *Monte Carlo Meth. and Appl.*, 9(2):93–133, 2003.
- [29] J-P. Minier, R. Cao, and S.B. Pope. Comment on the article ”an effective particle tracing scheme on structured/unstructured grids in hybrid finite volume/pdf monte carlo methods” by li and modest. *J. Comput. Phys.*, 186:356–358, 2003.
- [30] S.B. Pope. Particle method for turbulent flows: integration of stochastic model equations. *Journal of Computational Physics*, 117:332–349, 1995.
- [31] T. Ishima, J. Borrée, P. Fanouillère, and I. Flour. Presentation of a data base: confined bluff body flow laden with solid particles. *9th workshop on two-phase flow predictions*, Martin-Luther-Universität, Halle-Wittenburg, Germany, April 13-16 1999.
- [32] B.E. Launder, G.J. Reece and W. Rodi. Progress in the development of a Reynolds stress turbulence closure. *J. Fluid Mech*, 68:537, 1975.
- [33] B.E. Launder. Second-moment closure: present.. and future?. *Int.J.Heat Fluid Flow*, 10(4):282, 1989.

	CPU time for 1000 nodes/time step	CPU time for 1000 particles/time step
Eulerian solver	0.20 s	
Lagrangian solver		0.17 s

Table 1: Computational performances

List of Figures

1	Fluid element and particle paths	16
2	Mean fluid and particle paths	17
3	Sketch of the algorithm for one time step	17
4	The 'Hercule' experimental setup. The mean streamlines are shown for the fluid (solid lines) and the particles (dashed lines). Two stagnation points in the fluid flow can be observed (S_1 and S_2). Experimental data is available for radial profiles of different statistical quantities at five axial distances downstream of the injection ($x = 0.08, 0.16, 0.24, 0.32, 0.40 m$) (experimental data is also available on the symmetry axis).	18
5	Mean fluid velocity along the axis in single and two-phase flow.	19
6	Profiles of axial particle velocity along the axis (mean and fluctuating velocities)	19
7	Mean axial fluid velocity in two-phase simulation	20
8	Profiles of mean axial particle velocity	21
9	Profiles of mean radial particle velocity	22
10	Profiles of axial particle fluctuating velocity	23

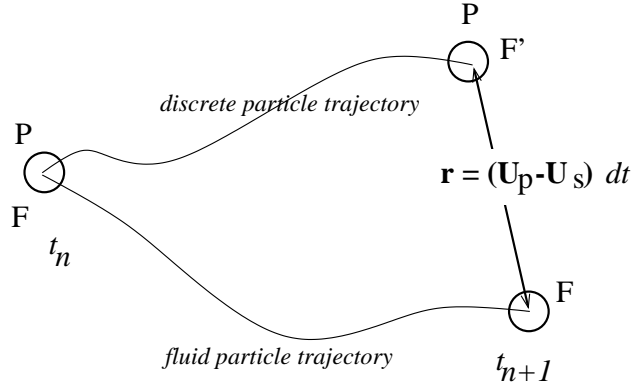


Figure 1: Fluid element and particle paths

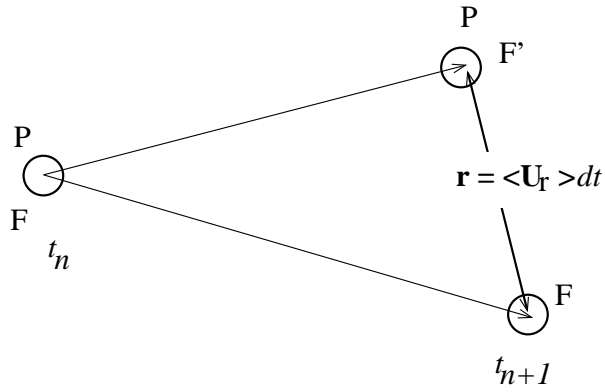


Figure 2: Mean fluid and particle paths

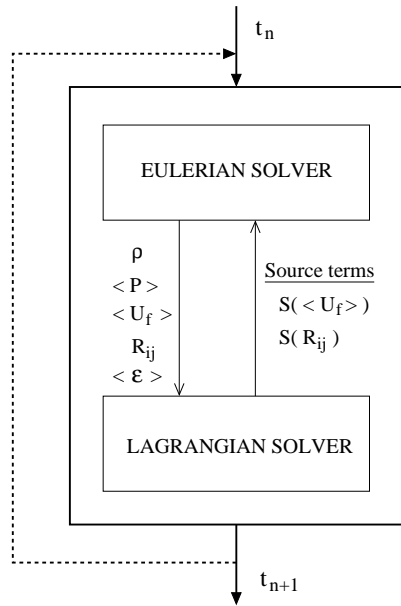


Figure 3: Sketch of the algorithm for one time step

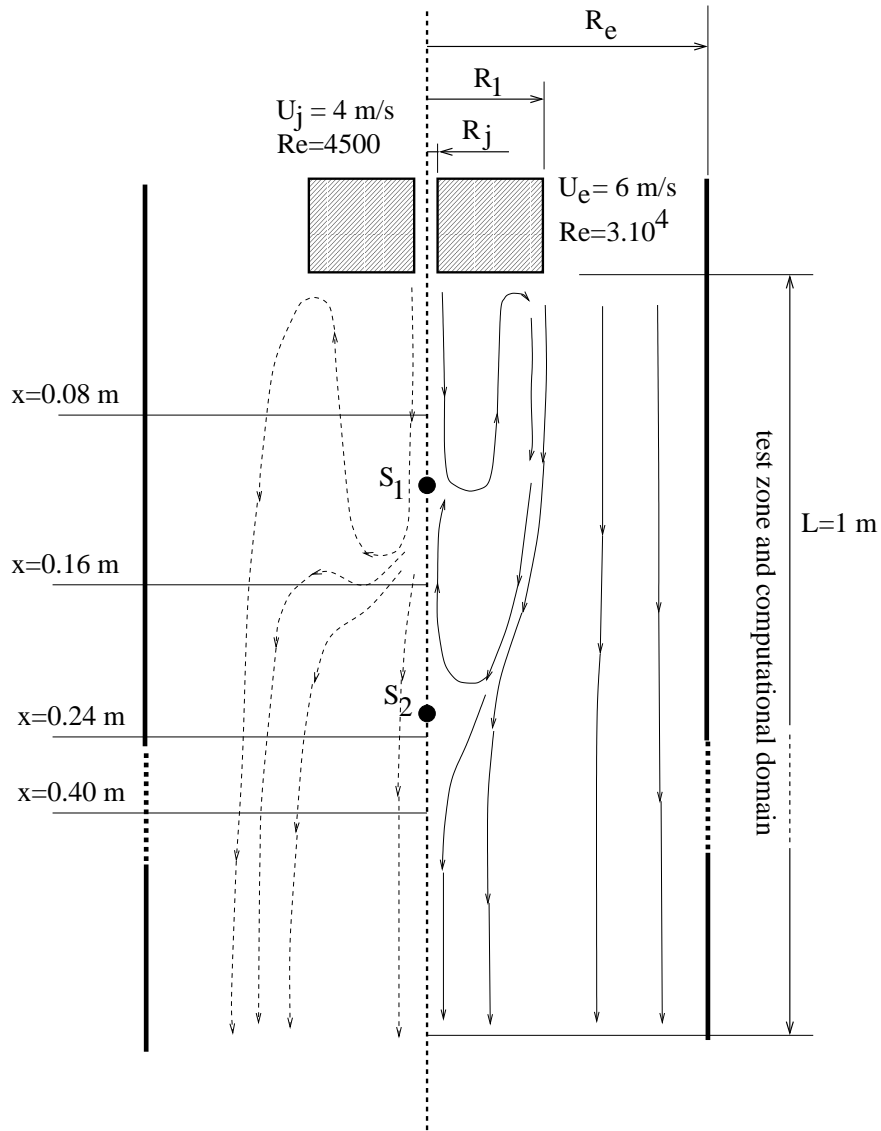


Figure 4: The 'Hercule' experimental setup. The mean streamlines are shown for the fluid (solid lines) and the particles (dashed lines). Two stagnation points in the fluid flow can be observed (S_1 and S_2). Experimental data is available for radial profiles of different statistical quantities at five axial distances downstream of the injection ($x = 0.08, 0.16, 0.24, 0.32, 0.40\text{ m}$) (experimental data is also available on the symmetry axis).

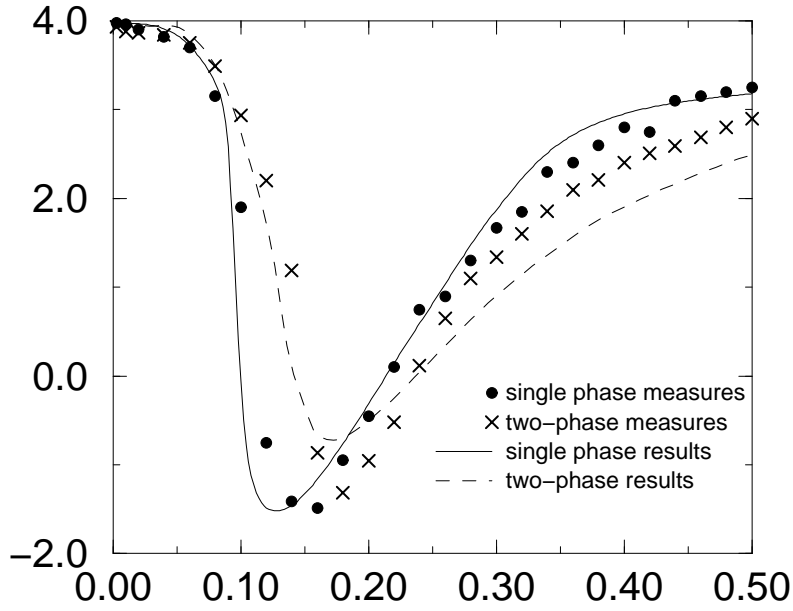


Figure 5: Mean fluid velocity along the axis in single and two-phase flow.

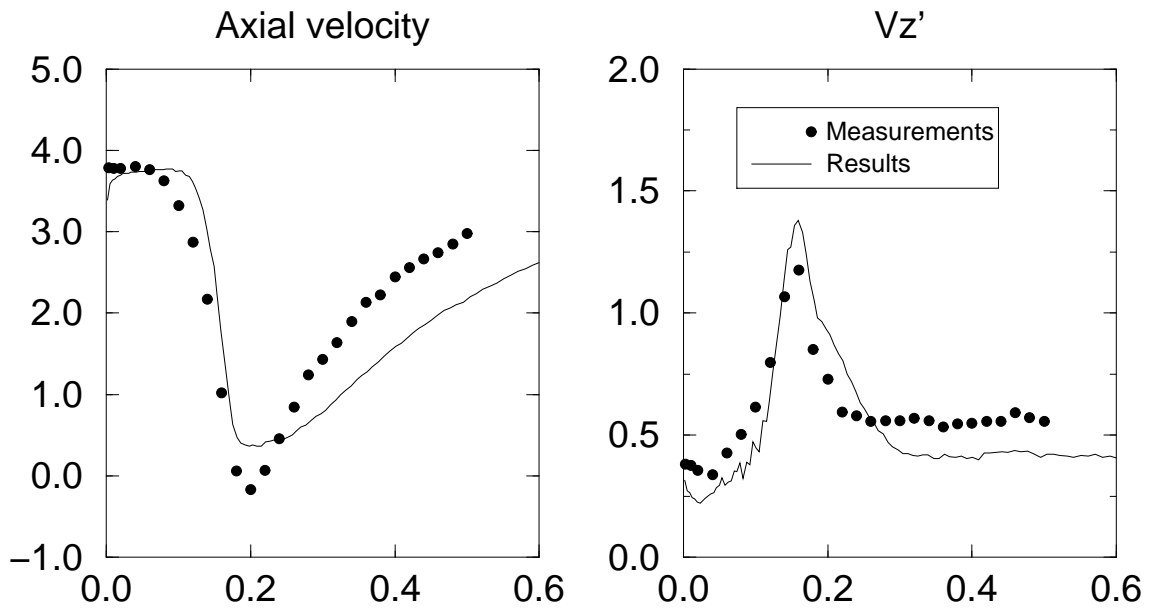


Figure 6: Profiles of axial particle velocity along the axis (mean and fluctuating velocities)

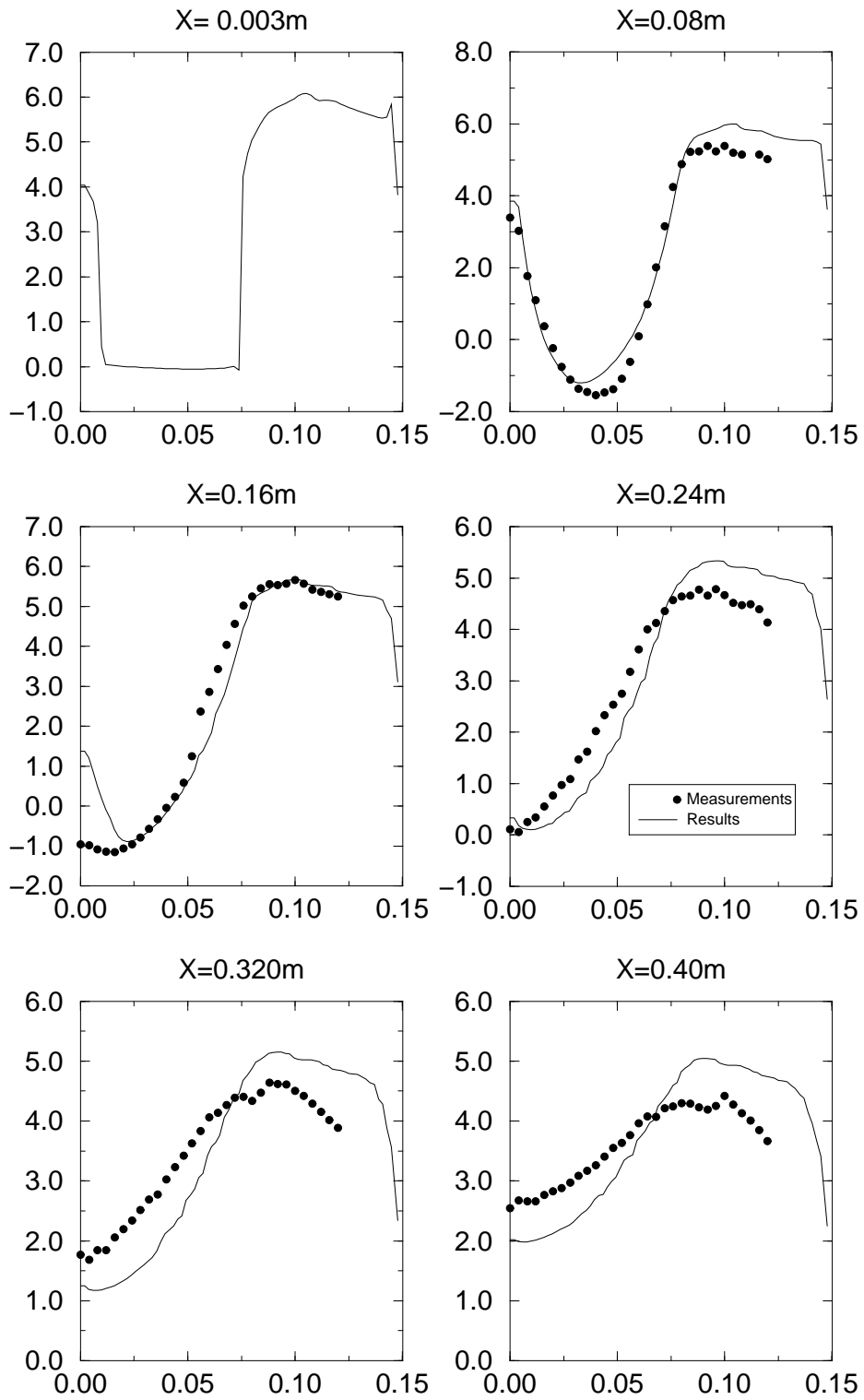


Figure 7: Mean axial fluid velocity in two-phase simulation

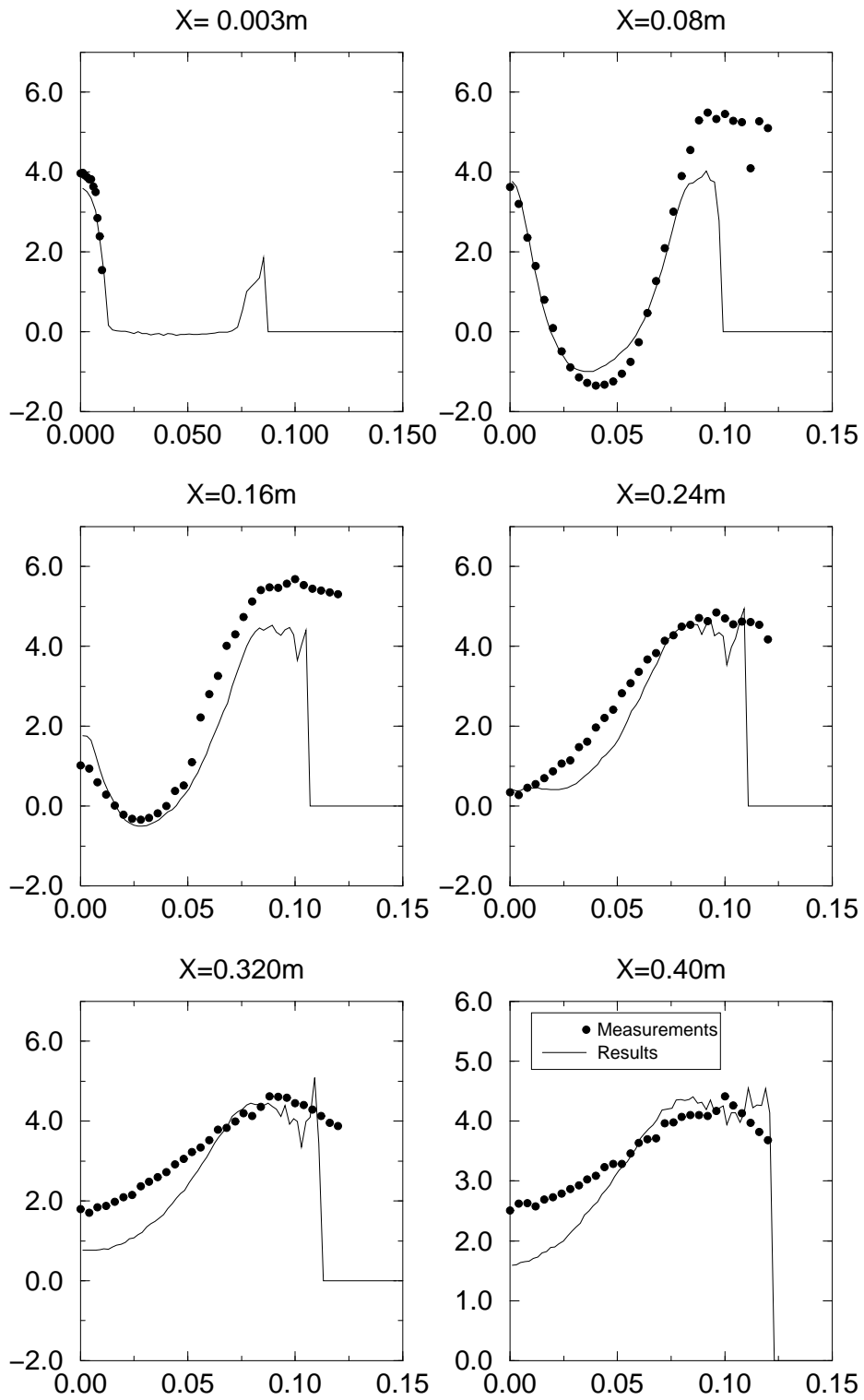


Figure 8: Profiles of mean axial particle velocity

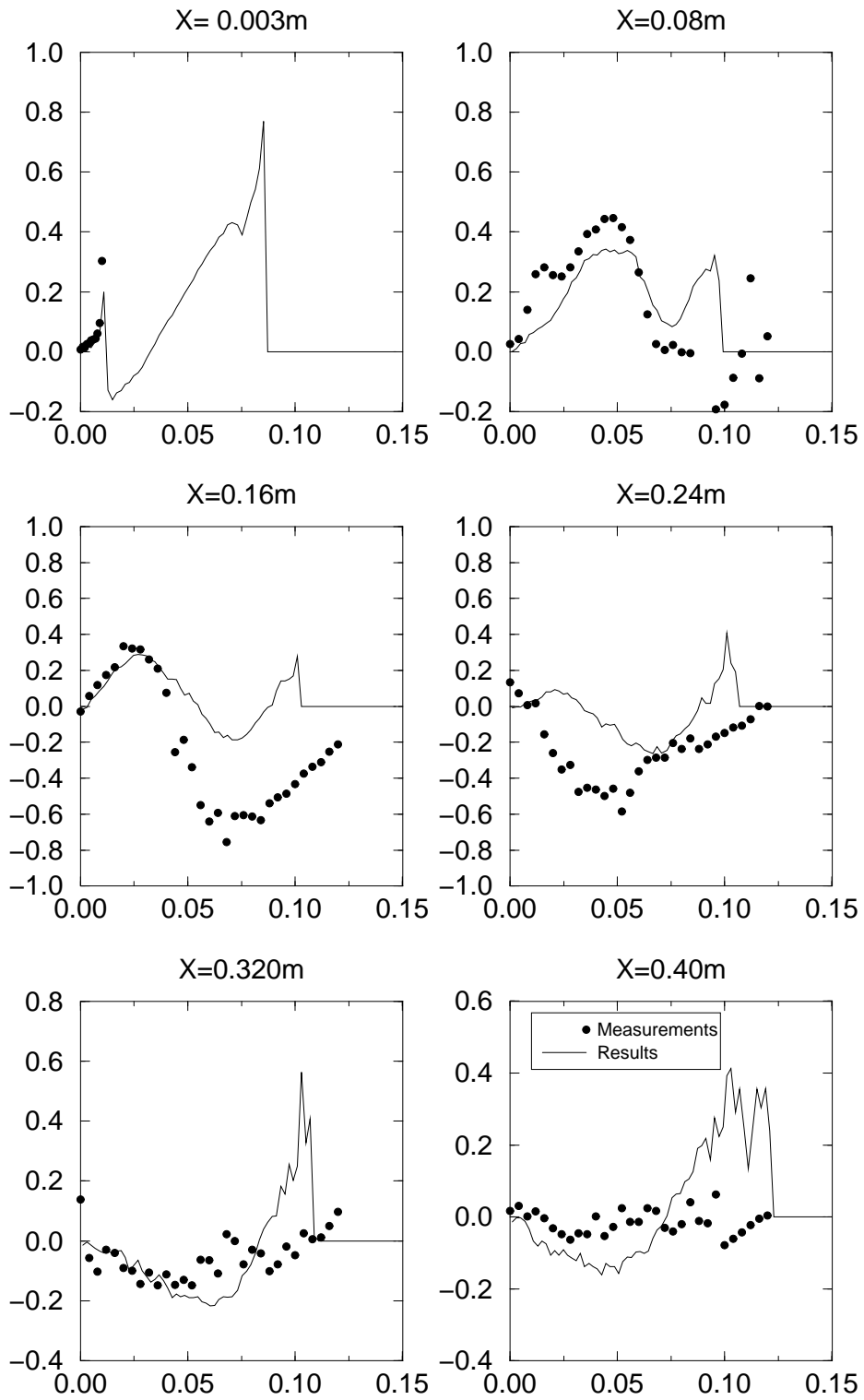


Figure 9: Profiles of mean radial particle velocity

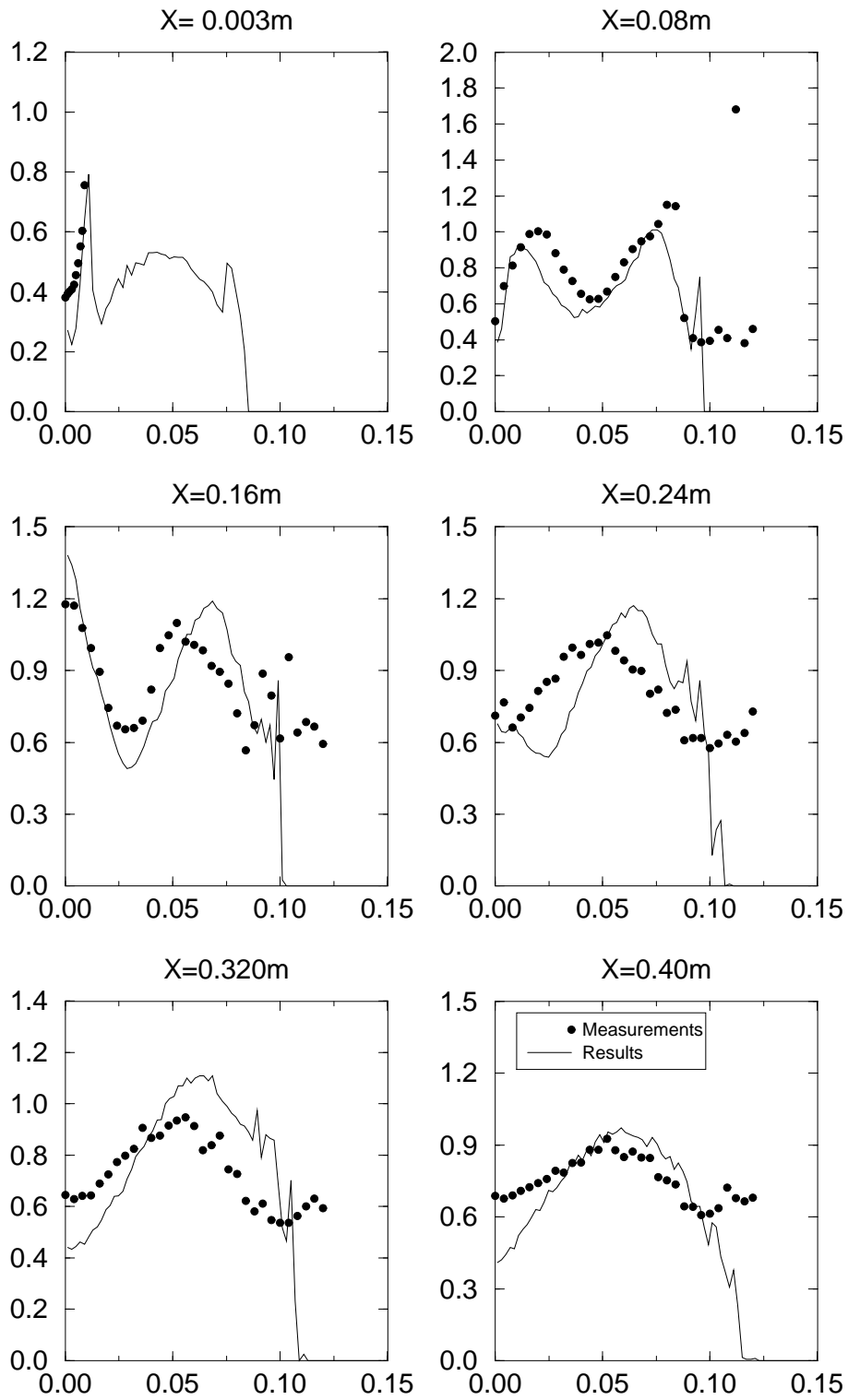


Figure 10: Profiles of axial particle fluctuating velocity